The 9th European Congress on Computational Methods in Applied Sciences and Engineering
ECCOMAS Congress 2024
3 – 7 June 2024, Lisboa, Portugal

BRICK MASONRY UNIT'S SPATIAL DYNAMIC MODULUS CHARACTERIZATION THROUGH IMPACT EXCITATION AND ULTRASONIC PULSE VELOCITY TEST

ABAYOMI P. OWOEYE[*], THOMAS DE'LARRARD[*], ZAKARIA DJAMAI[*] AND FREDERIC DUPRAT[*]

[*] Université de Toulouse; INSA, LMDC (Laboratoire Matériaux et Durabilité des Constructions); 135, avenue de Rangueil; F-31 077 Toulouse Cedex 04, France.
e-mail: lmdc@insa-toulouse.fr, www.lab-lmdc.fr

Key words: Uncertainty Propagation, Non-Destructive Testing, Mechanical Properties, Brick Masonry.

Summary. *Brick masonry is heterogeneous, consisting of unit brick and mortar, which govern its global behavior. However, due to the variability in the property of unit brick and mortar, there is usually a variability in the mechanical properties of brick masonry structure. For preservation, rehabilitation, uncertainty quantification, and probability structural integrity assessment, this variability in mechanical property is not easily assessable using static destructive tests. To address this problem, the nondestructive testing method was proposed to characterize the properties of brick masonry constituents. The test involved Impulse Excitation Technique (IET) and Ultrasonic Pulse Velocity (UPV) tests performed on masonry brick constituents classified based on varying sizes. IET was used to assess the possible global inconsistency of the constituent dynamic properties within a specimen, and the spatial variation of the dynamic elastic properties within the specimen was investigated using the UPV test results. The correlation of the average test result of the nondestructive dynamic modulus of elasticity with an existing static elastic modulus of the same material was explored and used for global characterization of the static modulus of elasticity within the specimen. It was observed that both nondestructive test results presented coherent and correlated results. The coherence of the IET and UPV allow for the global characterization of the constituents' static properties using both IET and UPV and for the spatial characterization based on the result obtained from the UPV test result.*

1 INTRODUCTION

Studying the mechanical properties of brick masonry is crucial to ensure the safety and durability of brick masonry structures. The mechanical properties of brick masonry govern the behavior of masonry structures, which depends on the mechanical properties of its constituents. However, owing to the variability in the properties of brick masonry constituents (unit brick, joint interface, and mortar), there is usually variability in the mechanical properties of the brick masonry structure. The common experimental approach adopted to study these properties can be classified as either destructive (mainly achieved by static testing) or nondestructive (achieved mainly by dynamic testing) testing of the brick masonry. However, for preservation,

rehabilitation, uncertainty quantification, and probability structural integrity assessment, the variability in the mechanical properties of brick masonry is not easily assessed using static destructive testing approach.

Therefore, with regards to mechanical property variation within the constituents of brick masonry and the masonry structure, the dynamic method of characterization provides an alternative to the static destructive testing due to its ability to provide faster, variable nondestructive results [1]. The dynamic method of characterization, which is based on the mechanical vibration of the brittle material microstructure on a microscopic scale, has gained attention in recent years for the characterization of brick masonry mechanical properties [2]. Most of these characterizations are based on global observations, however, the main mechanical properties of brick masonry, such as shear modulus, elastic modulus, shear strength, and compressive strength, exhibit significant degree of variability within the properties of its constituents, which defines its global behavior [3].

The dynamic testing techniques which made use of equipment that is nowadays widely used in construction industries and hence relatively accessible are the Impulse Excitation Technique (IET) and Ultrasonic Pulse Velocity (UPV) [4]. UPV testing is a widely used method for non-destructive evaluation of structural uniformity and quality, while IET testing uses accelerometers and data acquisition systems to monitor the dynamic response of structures like bridges and towers [5]. The IET and UPV techniques can capture global and spatial property variations within the material respectively.

As part of an ongoing program to access the probabilistic behavior of brick masonry, this study aims to evaluate the potential global and spatial dynamic properties of unit brick masonry categorized into sizes, explore the consistency of both the global and spatial dynamic properties, and identify a possible empirical correlation with reference to existing static properties for similar bricks within the scope of existing literature.

Therefore, to appraise the potential effect of unit brick size and homogeneity on its dynamic properties, IET technique was used to evaluate the global dynamic properties of bricks grouped into categories according to their sizes. This is then followed by exploiting the potential spatial variability of the dynamic properties within selected complete bricks using UPV testing techniques. For most structural analysis, it is common to use the statically determined properties instead of dynamic properties since the former is more representative of most loading conditions. Therefore, for the purpose of probability analysis and property uncertainty quantification, the consistencies of the global and spatial variable dynamic properties allow for a parallel correlation with existing static property obtained for similar brick.

2 MATERIALS SELECTION AND PREPARATION

The experimental campaign and dynamic properties field characterization of clay brick samples like those commonly used in historic buildings in Toulouse, France, was explored. A typical brick size as manufactured from the quarry is 420×210×50 mm^3. The bricks were selected and categorised according to sizes and presented in **Table 1**. Category A are complete sized brick sample, while categories B and C are extract from complete sized brick by dividing a complete sized brick into two along its length (Y-direction) and width (X-direction) respectively **Figure 1**. Categories B and C cutting were carefully achieved by a means of wet cutting machine to preserve the integrity of the parent brick. The purpose of size classification

is to assess the possible effect of brick size on the output of IET.

After selection and categorization, the surfaces of each brick sample were then regularised by polishing to maintain uniform dimension within the sample as well as improve the contact surface and accuracy of UPV testing. This is followed by air oven drying at 90°C until a constant mass is achieved.

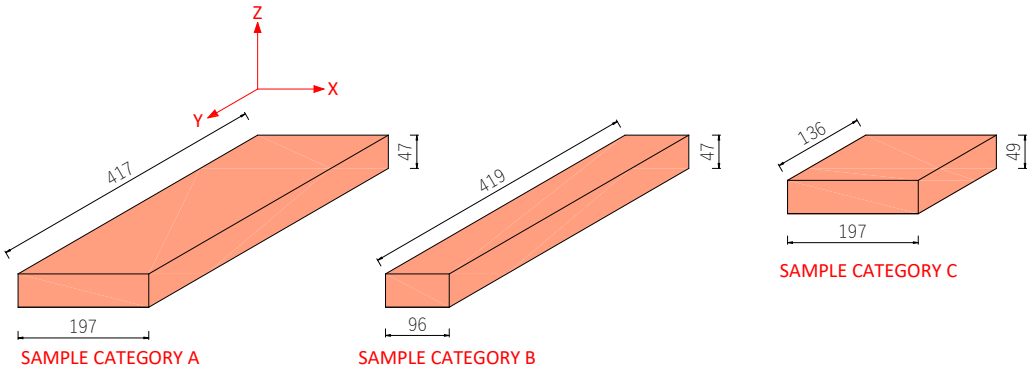

Figure 1: Brick samples categorized by size.

Table 1: Sample categories of bricks tested

	Category A	Category B	Category C
Number of samples	9	9	8
Average Unit weight (g)	7460	3760	2420
Average Length, mm (Direction Y)	417	419	136
Average Width, mm (Direction X)	197	96	197
Average Thickness, mm (Direction Z)	50	50	50

Lastly, for accurate positioning of transducers during UPV experiment, placement of the elastomeric support, location of receiver microphone and point of impact for the IET, the samples were marked based on the required testing procedure.

3 METHODOLOGY & THEORY

3.1 Impulse excitation technique (IET)

The IET testing method measures the fundamental resonant frequency of test sample with suitable geometry by exciting the samples mechanically using a single elastic strike with an impulse tool. Depending on the mode of excitation and boundary conditions imposed by the test set-up, the fundamental flexural (in-plane and out of plane), longitudinal and tortional frequencies of the sample can be measured. Established guidelines including ASTM E1876, ASTM C215 and ASTM C1259 [6–8] describe the specification on sample dimension, test set ups and procedures, and expressions relating fundamental resonant frequencies to dynamic properties. Depending on frequency of interest as shown in **Figure 2**, the procedure involves

setting up the sample on an elastomeric material support and exciting it at an appropriate location while a receiver transducer (microphone sensor) collects the required signal for analysis.

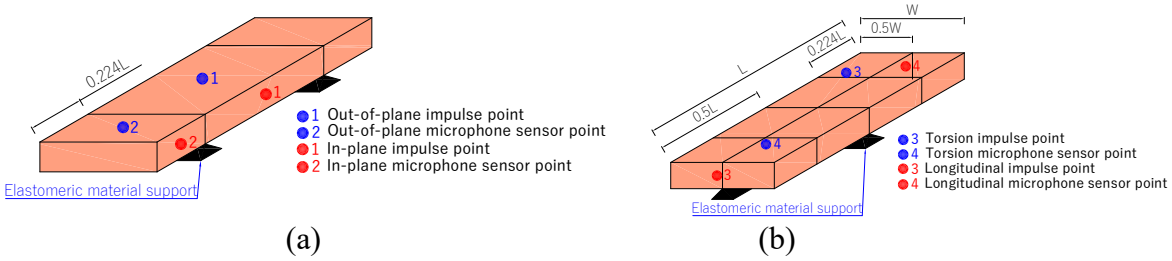

Figure 2: (a) Arrangement for out of plane and in-plane elastic dynamic modulus (b) Arrangement for shear and longitudinal dynamic modulus.

The dynamic properties of the test samples are related to the mechanical resonant frequencies, geometry and mass as follows:

i. Dynamic Young's Modulus, E (Pa)

a. From the fundamental flexure frequency, f_f (Hz) of a rectangular bar.

$$E = 0.9465\left(\frac{mf_f^2}{b}\right)\left(\frac{L^3}{t^3}\right)T_1 \tag{1}$$

Where m is the mass of the bar (g), b is the width of the bar (mm), L is the length of the bar (mm), t is the thickness of the bar (mm), T_1 is a correction factor for fundamental flexural mode to account for Poisson's ratio, t and L.

b. From the fundamental longitudinal frequency, f_l (Hz) of a slender bar with rectangular cross-section.

$$E = \frac{4Lmf_l^2}{bt} \tag{2}$$

ii. Dynamic Shear Modulus, G (Pa) from the fundamental torsional frequency, f_t (Hz) of a rectangular bar.

$$G = \frac{4Lmf_t^2}{bt}\left[\frac{B}{(1+A)}\right] \tag{3}$$

Where B and A are correction factors for fundamental torsional mode to account for b and t.

iii. Poisson's ratio,

$$\mu = \left(\frac{E}{2G}\right) - 1 \tag{4}$$

The dynamic properties (flexural, longitudinal and shear dynamic modulus of elasticity) of each sample in all categories were estimated from the average of 5 consecutive readings of the corresponding fundamental resonant frequencies for each experimental set up.

3.2 Ultrasonic pulse velocity (UPV)

UPV testing makes used of mechanical vibration consisting of longitudinal wave and shear waves which propagate in gases, liquid, and solids. The longitudinal waves also known as the compression waves or Primary waves (P-waves) are waves with particle displacement in the direction of the wave propagation, while the shear waves also known as transvers wave or Secondary waves (S-waves) are waves with particles displacement normal to the direction of wave propagation **Figure 3**.

The basic theoretical concept of waves propagation in isotropic homogeneous elastic media define the equation relating the velocity of propagation of a longitudinal wave ($V_p, m/s$) and the shear wave ($V_s, m/s$) to the material density ($\rho, kg/m^3$), Young's Modulus (E), Poisson's ratio (μ) and modulus of rigidity or shear modulus (G) as:

$$E = \frac{\left[\rho V_s^2(3V_p^2 - 4V_s^2)\right]}{(V_p^2 - V_s^2)} \tag{5}$$

$$\mu = \frac{(V_p^2 - 2V_s^2)}{\left[2(V_p^2 - V_s^2)\right]} \tag{6}$$

$$G = \rho V_s^2 \tag{7}$$

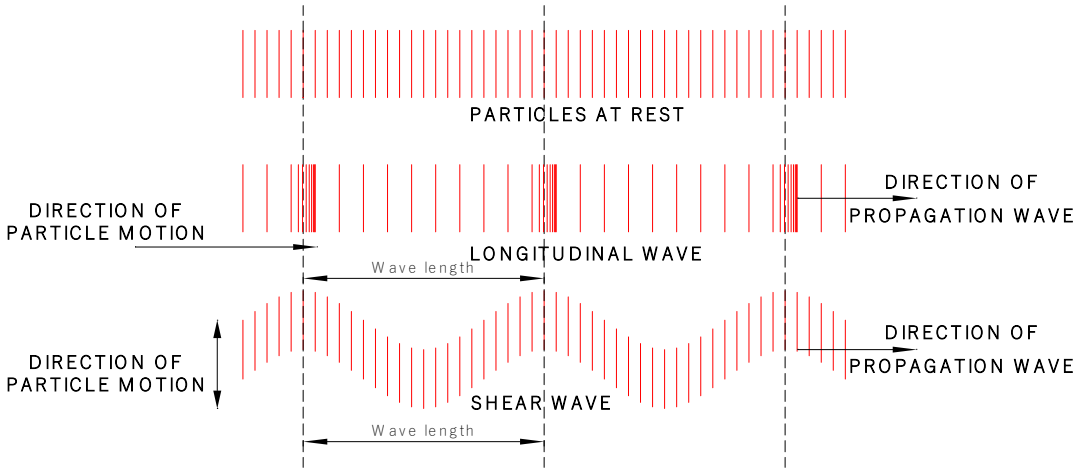

Figure 3: Particle displacement and direction of wave propagation through a homogenous elastic body.

3.2.1 UPV experimental principle

The use of ultrasonic waves traveling through a medium is most widely used for rocks and concrete testing and as such there are well established guidelines including ASTM D2845 and ASTM C597 [9,10]. Although ASTM C597, described a procedure using only the P-wave assuming a prior knowledge of concrete Poisson's ratio, ASTM D2845, describes the equipment and procedures for laboratory measurements of P-waves and S-waves pulse velocities and the determination of corresponding ultrasonic elastic constants. The procedure makes use of a pulse generator, a pair of shear transducers (a transmitter and a receiver), and

an oscilloscope as shown in **Figure 4**. The testing procedure as described in ASTM D2845 was adopted for this study.

5 samples collected from category A (Sample A1-A5) were marked as schematically displayed in **Figure 5** (a). Established on each sample are opposite alternating points of 4 across the length L-L (Fig 1, Y-Y direction), 12 across the width W-W (Fig 1, X-X direction) and 48 across the thickness, Fig. 1, Z-Z direction. The length, width, and thickness at each point across each paths indicated were measured and recorded. This is followed by measuring the pulse transit time of both P-waves and S-waves at least 3 times and the average transit time used in estimating the respective pulse velocity at that point. The P-waves travel the fastest and its transmission arrival time is detected relatively easy, followed by the S-waves **Figure 5** (b). It is to be noted that the S-waves arrival may be obscured due to reflections of the compression wave.

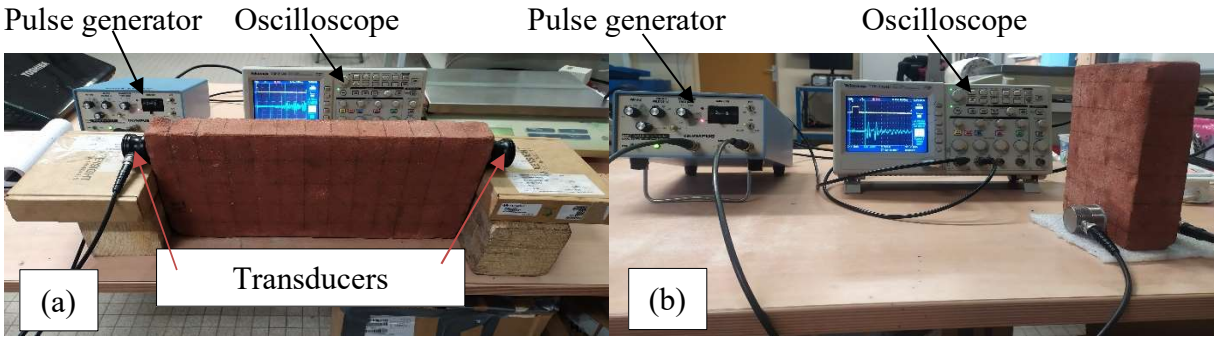

Figure 4: (a) UPV Measurement across length (b) UPV Measurement across thickness.

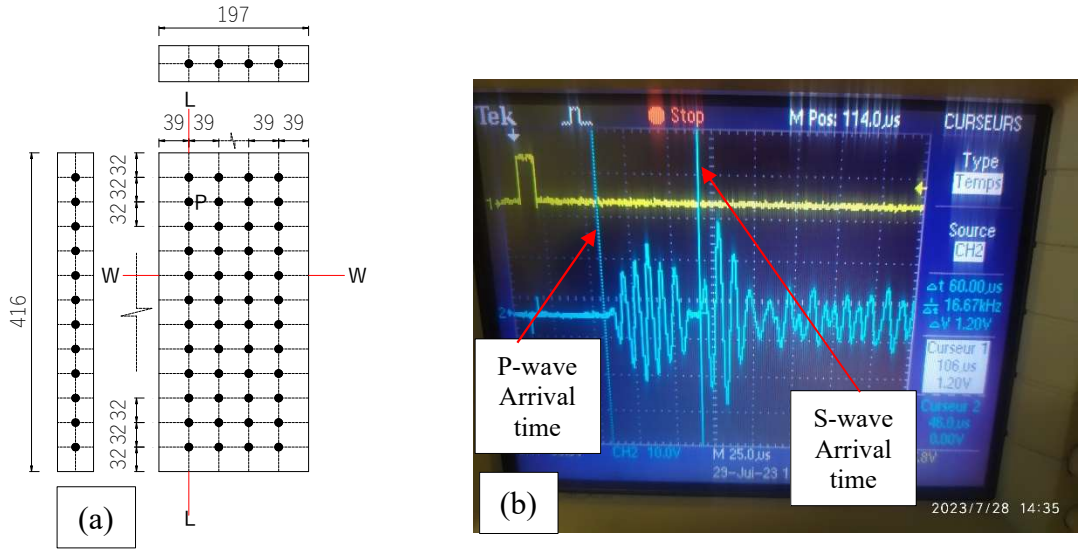

Figure 5: (a) Schematic marking of sample for UPV testing (b) Typical example of primary and secondary wave form.

Subsequently, the pulse velocity for both P-waves and S-waves was calculated using equation (8) and (9) the dynamic properties across each point was estimated using equations (5), (6) and (7).

$$V_p = \frac{l}{t_p} \tag{8}$$

$$V_s = \frac{l}{t_s} \tag{9}$$

Where $l: pulse\ travel\ distance, in\ m$, and $t_p, t_s: the\ average\ pulse\ travel\ time, in\ s$ for P-wave and S-wave respectively.

4 RESULTS

The results from each experimental campaign were analysed and discussed below. First the EIT results were discussed, which evaluate the global dynamic characteristics, followed by the UPV results which was aimed at characterising the spatial variation of the dynamic properties. The alphabet (A, B and C) of each category hereafter represents the categories in the tables presented below. The dynamic share modulus and the Poisson's ratio were estimated using the dynamic out of plane elastic modulus.

4.1 Global dynamic frequencies and elastic properties

As described earlier, depending on the frequency of interest, 5 consecutive readings of the corresponding fundamental resonant frequencies for each sample were recorded and the average was used to estimate the proportionate dynamic modulus of elasticity of that sample. With reference to the mode of the EIT experiment, the dynamic resonant frequencies were identify as f_{OP}, f_{IP}, f_L, and f_T, for dynamic out of plane, in plane, longitudinal, and torsional resonant frequency, while the dynamic elastic properties were identified as E_{OP}, E_{IP}, E_L, G, and PO for dynamic out of plane, in plane, longitudinal, share modulus, and dynamic Poisson's ratio respectively. All the fundamental frequencies measured (**Table 2** and **Figure 6**) were in the range of 702Hz for out of plane resonant frequency with a Coefficient of Variation (CV) of 3% to 7224Hz for longitudinal resonant frequency with a CV of 7%. It obvious from **Figure 6** which compare the average dynamic resonant frequency between each category of samples and equation 1, 2, 3, and 4, that length of a sample having the same thickness has a great influence on the fundamental resonant frequency of the sample, with the resonant frequency increasing with decrease in length.

Table 2: Range of global dynamic fundamental frequencies

	Dynamic out of plan flexural resonant frequency, f_{OP} (Hz)			Dynamic In plan flexural resonant frequency, f_{IP} (Hz)			Dynamic longitudinal resonant frequency, f_L (Hz)			Dynamic torsional resonant frequency, f_T (Hz)		
	A	B	C	A	B	C	A	B	C	A	B	C
Maximum	769	817	3324	2245	I413	5411	3448	3550	7224	984	1673	2948
Minimum	702	693	2750	1829	1167	4656	2887	2970	6002	877	1437	2513
CV	3%	7%	5%	7%	7%	5%	5%	6%	7%	4%	5%	5%

The elastic properties estimated from each EIT experimental procedures were presented in **Table 3** and **Figure 7**.

The dynamic modulus of elasticity ranges from approximately 11GPa to 17GPa with a maximum variation of 14% irrespective of the size of the sample or the mode of EIT test adopted. Similarly, the global share modulus of elasticity is approximately the same ranging from 5GPa to 7GPa with an approximate maximum variation of 8% across all the categories of sample size.

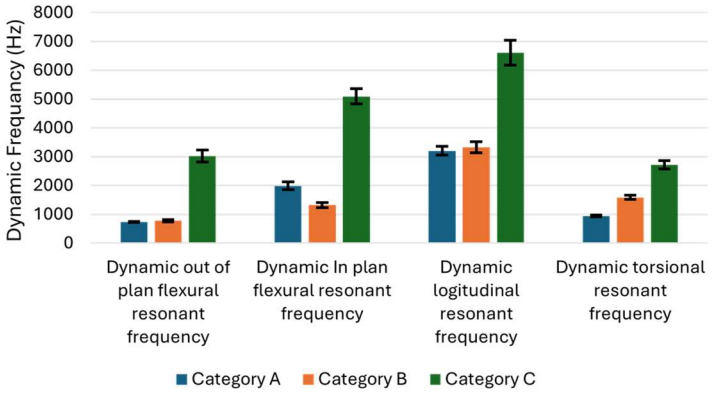

Figure 6: Average dynamic resonant frequency based EIT testing technique.

Table 3: Range of dynamic modulus of elasticity and share

	Dynamic out of plan flexural modulus of elasticity, E_{OP} (GPa)			Dynamic In plan flexural modulus of elasticity, E_{IP} (GPa)			Dynamic longitudinal modulus of elasticity, E_L (GPa)			Dynamic share modulus of elasticity, G (GPa)		
	A	B	C	A	B	C	A	B	C	A	B	C
Maximum	15.72	16.78	16.99	16.18	15.88	14.75	15.7	16.36	14.85	6.873	6.409	6.667
Minimum	12.65	12.28	12.11	10.74	10.84	11.29	11.1	12.39	10.7	5.402	5.178	5.213
Average	14.05	14.48	14.35	12.56	13.66	13.20	13.60	14.57	12.69	6.229	5.800	6.072
CV	7%	10%	11%	14%	12%	10%	9%	10%	12%	7%	7%	8%
Experiment average	14.29			13.14			13.62			6.033		

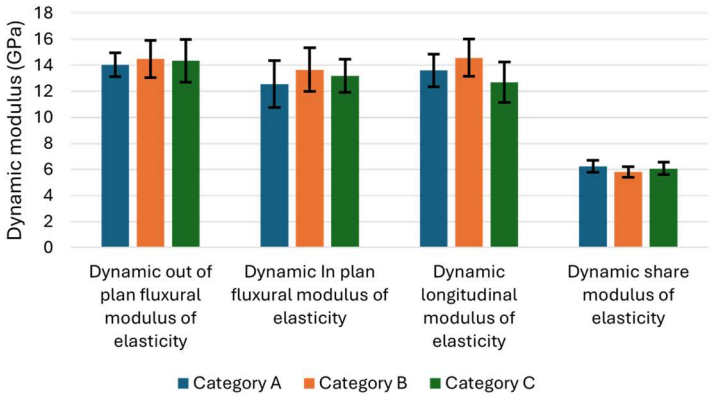

Figure 7: Average dynamic modulus of elasticity based on EIT testing technique.

4.2 Global Poisson's ratio

The dynamic Poisson's were estimated iteratively to satisfy equation 1, 3 and 4. **Table 4** and **Figure 8** present the range, variation, and average Poisson's ratio from each category of samples. The Poisson ratio averages for categories A, B, and C are 0.13, 0.25, and 0.18. However, it appears that there is considerable scatter in the Poisson's ratio, with the highest variability of 49% observed in Category A and the lowest variability of 20% observed in category B.

Table 4: Range of dynamic modulus of elasticity and share

	Dynamic out of plan flexural resonant frequency, f_{OP} (Hz)		
	A	B	C
Maximum	0.2656	0.3128	0.2739
Minimum	0.0498	0.1525	0.078
CV	49%	20%	31%

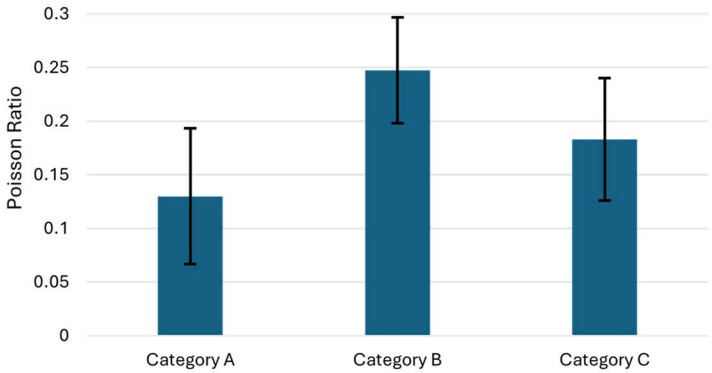

Figure 8: Average Poisson's Ratio based category of sample.

4.3 Spatial dynamic elastic properties

Figure 9 (a) and (b) compare the average dynamic moduli and share moduli estimated from both EIT and UPV testing for sample A1 – A5. Note that only one value of IET dynamic moduli were estimated for each sample, while 4, 12, and 48 UPV dynamic moduli were estimated across sample length, width, and thickness (**Figure 5** (a)), respectively for each sample.

The estimated IET dynamic moduli range from 11.13GPa to 15.69GPa with an average value of 14.24GPa for out of plane flexural modulus and 13.7GPa for longitudinal modulus, like the global average obtainable in **Table 3**. The UPV dynamic moduli ranges from 11.43GPa (CV = 6%) to 12.68GPa (CV = 8%) across the thickness, to the highest value of 12.82GPa (CV = 10%) across the length of the samples.

Similarly, the average IET share modulus ranges from 5.4GPa to 6.9GPa, while the average UPV share modulus ranges from 5.1GPa (CV = 7%) to 5.6GPa (CV = 8%).

Based on the direction of UPV measurement, the estimated dynamic modulus of elasticity was identified as $E_{UPV,L}$, $E_{UPV,W}$, and $E_{UPV,T}$ for dynamic modulus across the length, width, and

thickness of the sample respectively. Given that bricks are most often loaded in compression across their thickness, $E_{UPV,T}$ of each sample was compared with the other estimated dynamic modulus of elasticity and percentage difference varies from 1 – 27% (**Table 5**).

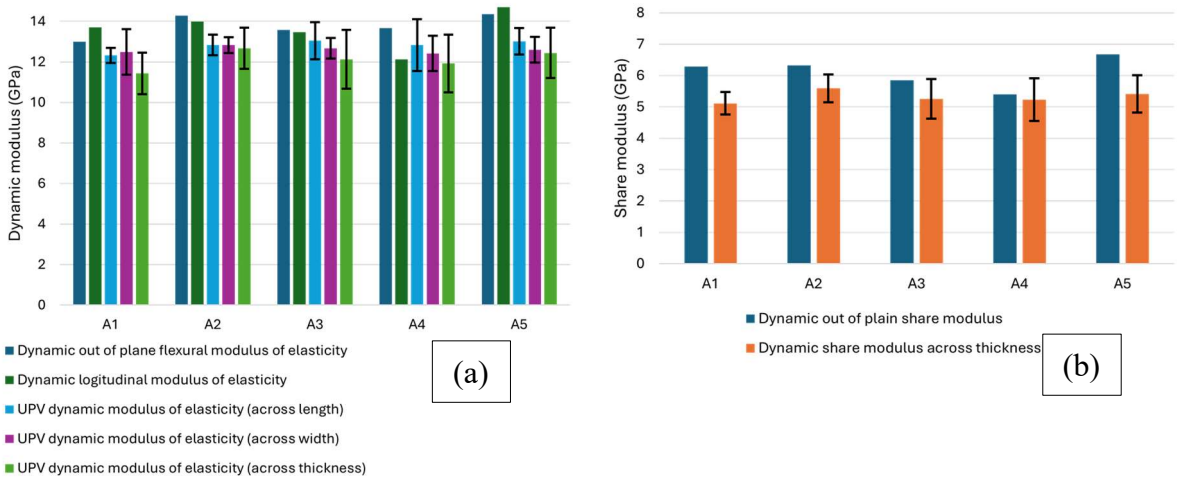

Figure 9: Average IET and UPV dynamic elastic and share moduli for sample A1 – A5 (a) Average dynamic elastic moduli (b) Average dynamic share moduli.

Table 5: Absolute relative percentage UPV dynamic elastic modulus across sample thickness

	$Abs\left(1-\frac{E_{OP}}{E_{UPV,T}}\right)\%$	$Abs\left(1-\frac{E_{L}}{E_{UPV,T}}\right)\%$	$Abs\left(1-\frac{E_{UPV,L}}{E_{UPV,T}}\right)\%$	$Abs\left(1-\frac{E_{UPV,W}}{E_{UPV,T}}\right)\%$
A1	23%	24%	8%	9%
A2	21%	10%	1%	5%
A3	12%	11%	8%	4%
A4	24%	4%	6%	4%
A5	18%	24%	5%	1%

5 DYNAMIC AND STATIC MODULUS CORRELATION

Makoond [11], proposed a linear relationship between the dynamic and static modulus of elasticity for masonry brick unit to include manufactured handmade unit bricks in molds. The static modulus of elasticity was related to the dynamic modulus by:

$$E_{ST} = 0.87E_{DY} \tag{10}$$

Where E_{ST} and E_{DY} are the corresponding static and dynamic modulus of the unit brick respectively.

Therefore, the global static modulus of elasticity estimated from the IET testing results (**Table 3**) are 12.4 GPa, 11.4 GPa, and 11.9 GPa for flexure out of plane, flexure in plane, and longitudinal modulus of elasticity.

The static modulus of elasticity has been previously measured for similar brick under the same manufacturing process. These results produce an average static modulus of 7.4 MPa with a considerable scatter between 4.9GPa and 12.6 GPa from simple compression test on extracted cylindrical samples [12].

For the spatial elastic properties and considering the 5 samples from category A, the UPV test results across thickness and their equivalent estimated static dynamic modulus of elasticity were presented in **Figure 10**. The estimated average static modulus of elasticity range between 9.9 GPa to 11.0 GPa.

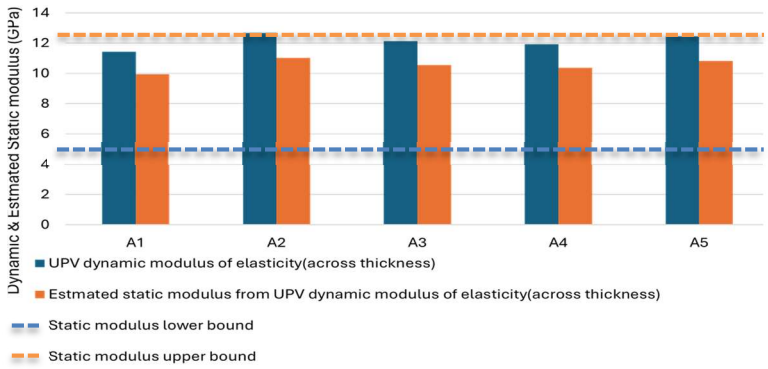

Figure 10: UPV dynamic modulus across thickness and equivalent estimated static modulus.

6 CONCLUSIONS

This article presents the possibility of estimating the spatial properties of masonry brick units from nondestructive testing. Two nondestructive testing techniques (IET and UPV) were employed to verify the global and spatial consistency of the material's elastic properties. The main conclusions drawn from the test results are as follows.

- The global dynamic elastic modulus estimated from the IET testing approximately varies between 13.14GPa to 14.26GPa, while the spatial variability of the elastic dynamic modulus from the UPV testing varies between 11.43GPa (CV = 6%) to 12.68GPa (CV = 8%) across the thickness of a sample.
- The IET global dynamic share modulus varies between 5.8GPa and 6.2GPa with an average value of 6GPa, while the spatial dynamic share modulus for a sample varies between 5.1GPa (CV = 7%) to 5.6GPa (CV = 8%).
- On average, the dynamic moduli estimated from the IET are greater than those estimated from the UPV testing. However, comparing the UPV dynamic modulus to all other forms of measured modulus, there exists a considerable consistency with relative variation between 1 – 24%.
- The estimated average static modulus of elasticity (9.9GPa - 11.0GPa), by and large, the static modulus of elasticity at each point within a sample brick, is within the range of existing static modulus for the same material (4.9GPa - 12.6GPa). Note that the result of the existing static modulus lower bound, as indicated in **Figure 10**, shows a low modulus compared to the estimated one. This may be attributed to the effect of loading. Such a decrease is expected and can be explained to be a result of the formation of cracks or internal micro-cracks in the brick under loading [13].

This work is part of an ongoing program at the LMDC laboratory, INSA, Toulouse to access the probabilistic behavior of brick masonry. Further works are ongoing to characterize the random field properties of estimated modulus of elasticity, estimate the spatial properties of

wall mortar component, propagate the spatial uncertainties into mechanical model and look at their effect in terms of reliability.

REFERENCES

[1] Domede N, Parent T, Guenser C, Boukham A, Morenon P, Issa-Ibrahim AS. Mechanical characterisation of the stones of Notre-Dame de Paris by in situ acoustic velocity measurement. Int J Rock Mech Min Sci 2024;175:105671. https://doi.org/10.1016/j.ijrmms.2024.105671.

[2] Dizhur D, Lumantarna R, Biggs DT, Ingham JM. In-situ assessment of the physical and mechanical properties of vintage solid clay bricks. Mater Struct 2016;50:63. https://doi.org/10.1617/s11527-016-0939-9.

[3] Croce P, Beconcini ML, Formichi P, Cioni P, Landi F, Mochi C, et al. Shear modulus of masonry walls: a critical review. Procedia Struct Integr 2018;11:339–46. https://doi.org/10.1016/j.prostr.2018.11.044.

[4] Makoond N, Pelà L, Molins C. Dynamic elastic properties of brick masonry constituents. Constr Build Mater 2019;199:756–70. https://doi.org/10.1016/j.conbuildmat.2018.12.071.

[5] McCann DM, Forde MC. Review of NDT methods in the assessment of concrete and masonry structures. NDT E Int 2001;34:71–84. https://doi.org/10.1016/S0963-8695(00)00032-3.

[6] ASTM C215-19 - Standard Test Method for Fundamental Transverse, Longitudinal, and Torsional Resonant Frequencies of Concrete Specimens | GlobalSpec n.d. https://standards.globalspec.com/std/13946813/ASTM%20C215-19 (accessed March 25, 2024).

[7] ASTM E1876-21 - Standard Test Method for Dynamic Young's Modulus, Shear Modulus, and Poisson's Ratio by Impulse Excitation of Vibration n.d. https://webstore.ansi.org/standards/astm/astme187621 (accessed March 25, 2024).

[8] ASTM-C1259 - Standard Test Method for Dynamic Young's Modulus, Shear Modulus, and Poisson's Ratio for Advanced Ceramics by Impulse Excitation of Vibration | Document Center, Inc. n.d. https://www.document-center.com/standards/show/ASTM-C1259 (accessed March 25, 2024).

[9] ASTM D2845-08 - Standard Test Method for Laboratory Determination of Pulse Velocities and Ultrasonic Elastic Constants of Rock (Withdrawn 2017) | GlobalSpec n.d. https://standards.globalspec.com/std/3832891/astm-d2845-08 (accessed March 25, 2024).

[10] ASTM C597-16 - Standard Test Method for Pulse Velocity Through Concrete | GlobalSpec n.d. https://standards.globalspec.com/std/3861326/ASTM%20C597-16 (accessed March 25, 2024).

[11] Makoond N, Cabané A, Pelà L, Molins C. Relationship between the static and dynamic elastic modulus of brick masonry constituents. Constr Build Mater 2020;259:120386. https://doi.org/10.1016/j.conbuildmat.2020.120386.

[12] TARIFA N. Renforcement de la maçonneries historique par les composites TRM. Institut National des Sciences Appliquées de Toulouse, 2023.

[13] Miranda L, Guedes J, Rio J. Stone Masonry Characterization Through Sonic Tests 2010.